Supporting Information

Figure S1 shows the complex viscosity of polymers used in this study. It was measured as below. Polymers, as received, were melt-kneaded for 5 min at 190 °C under a nitrogen atmosphere using a conical twin-screw micro-compounder (MC15, Xplore) at 200 rpm to remove the shear history. A small piece (0.5–1.0 g) of the extruded sample was placed in a steel mould (ϕ 25 mm diameter circle, 0.9 mm thickness) between two sheets of polyimide film (Kapton 5 mil, Dupont). The sample was then preheated at 190 °C for 2 min in a hydraulic press (Carver, Inc., Wabash) without applied pressure and pressed at 190 °C for 1 min under 100–200 kg clamp force. Then the sample was immediately cooled to room temperature in a water-cooled press. Rheological tests were performed at 190 °C in a dry nitrogen atmosphere using a 25 mm parallel plate, rotational rheometer (MCR302 by Anton Paar). The frequency sweep tests were performed at a strain of 5%. Samples were kept at 190 °C for 3 min in the rheometer before performing the tests.

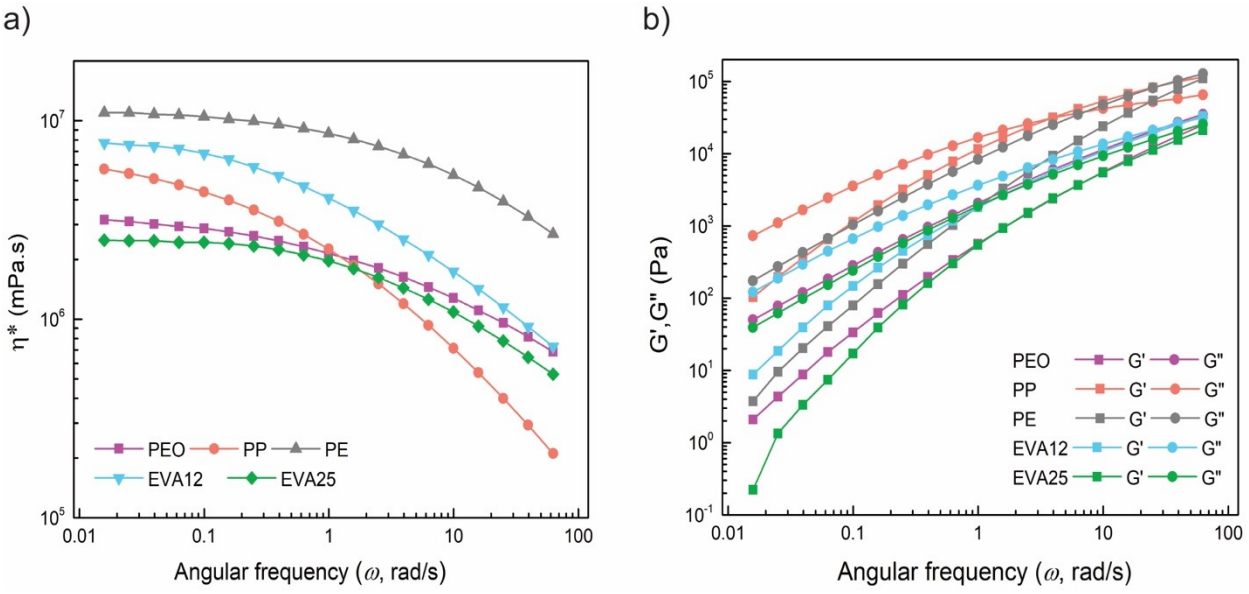

Figure S1. a) Complex viscosity vs. angular frequency and, b) G',G" vs. angular frequency graphs of the polymer components.

Table S1 shows the result of the estimation of the spreading coefficient λ of the ternary polymer blend, the interfacial tension of the binary polymer blends, and the results of the estimation of the wetting coefficient of the blends. Each material's surface tension value and temperature coefficient are extracted from literatures[s1−s6].

Table S1. The surface tension of polymer/silica, interfacial tension of the binary blends, the ternary blend's spreading coefficient, and the blends' wetting coefficient.

	Surface tension (mN m^{-1}) at 200 °C			Interfacial tension (Owens & Wendt) γ_{12}	Spreading coeff (mN m^{-1})			Wetting coeff
	γ	γ^d	γ^p		$\lambda_{\text{PE EVA PEO}}$	$\lambda_{\text{EVA PE PEO}}$	$\lambda_{\text{EVA PEO PE}}$	ω
PE	26.6	26.6	0.0					
PP	16.4	16.3	0.1					
EVA12	25.7	22.8	2.9					
EVA25	35.43	34.18	1.25					
PEO	30.7	22.2	8.5					
SNP	48.8	27.5	21.3					
PE/EVA12				3.1				
PP/EVA12				2.7				
PEO/EVA12				1.5				
PE/SNP				21.3				
PP/SNP				19.9				
PEO/SNP				3.2				
EVA12/SNP				8.7				
EVA25/SNP				12.6				
PE / EVA 12/ PEO					4.2	-10.2	-7.1	
PE/EVA25/PEO					2.5	-5.9	-11.5	
PE / EVA / SNP								-4.1 (SNP prefers EVA phase)
PE / PEO / SNP								-2.1 (SNP prefers PEO phase)
PP/EVA/SNP								-3.17 (SNP prefers EVA phase)
EVA / PEO / SNP								-3.6 (SNP prefers PEO phase)

Figure S2 shows the overlap of PEO and SNP channels of the quaternary blends, indicating the selective localization of nanoparticles within the PEO phase.

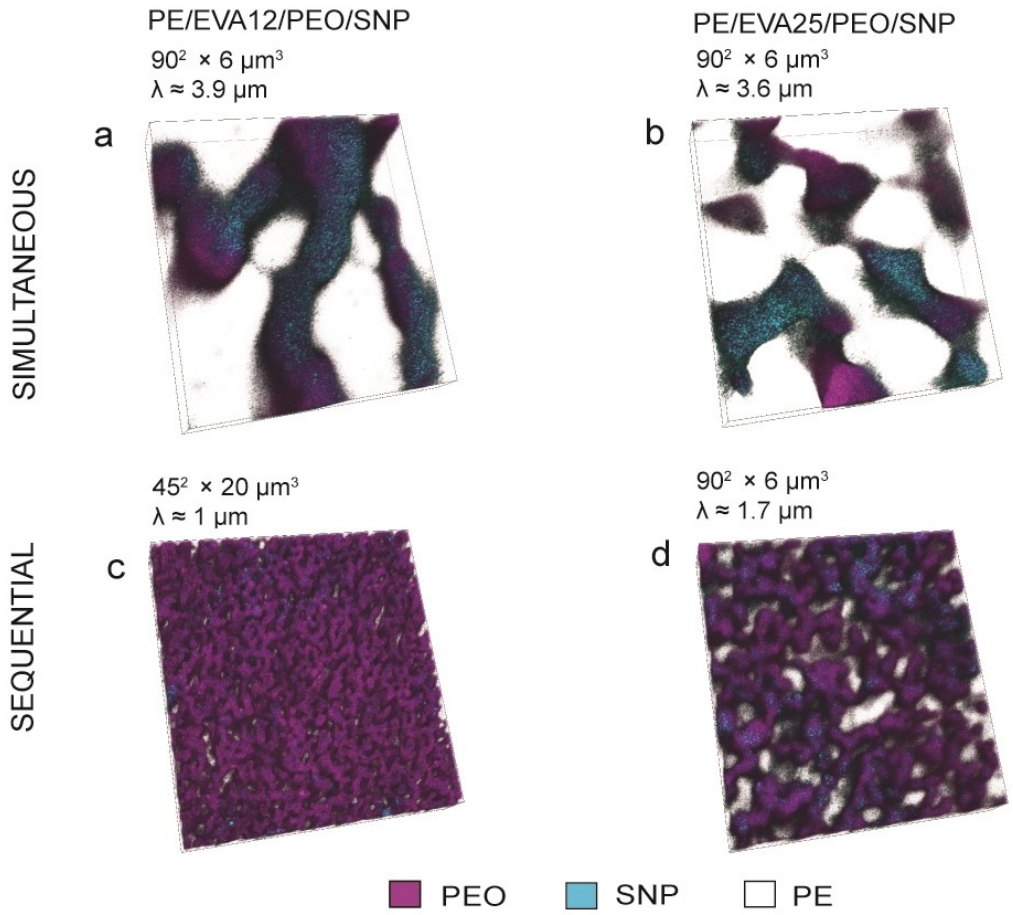

Figure S2. PEO and SNP channels of the simultaneously and sequentially blended PE/EVA12/PEO/SNP and PE/EVA25/PEO/SNP quaternary blends.

Figure S3 illustrates the average characteristic size of the neat polymer blends, co-continuous and tri-continuous polymer blend nanocomposites. Each characteristic size is the average of four separate batches of blend systems.

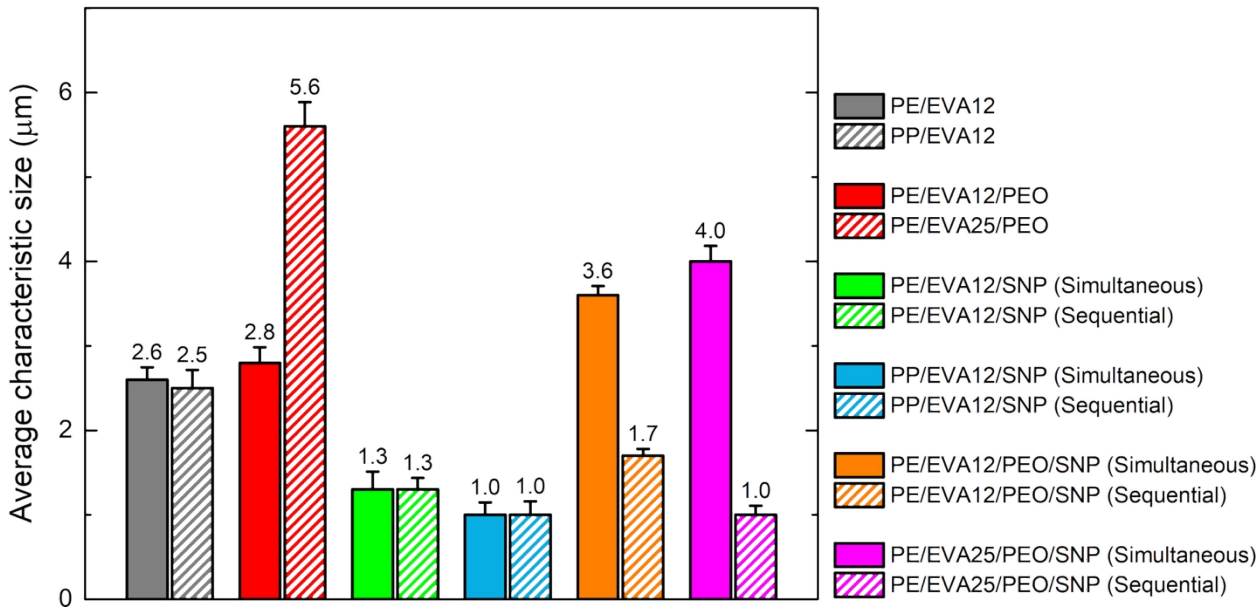

Figure S3. Average characteristic size of neat polymer blends, co-continuous and tri-continuous blend nanocomposites from four different samples.

Figure S4 shows LSCM images of EVA/PEO (50/50 vol%) blends filled with 30 wt% (28 vol% to PEO) SNPs after 30 min melt annealing.

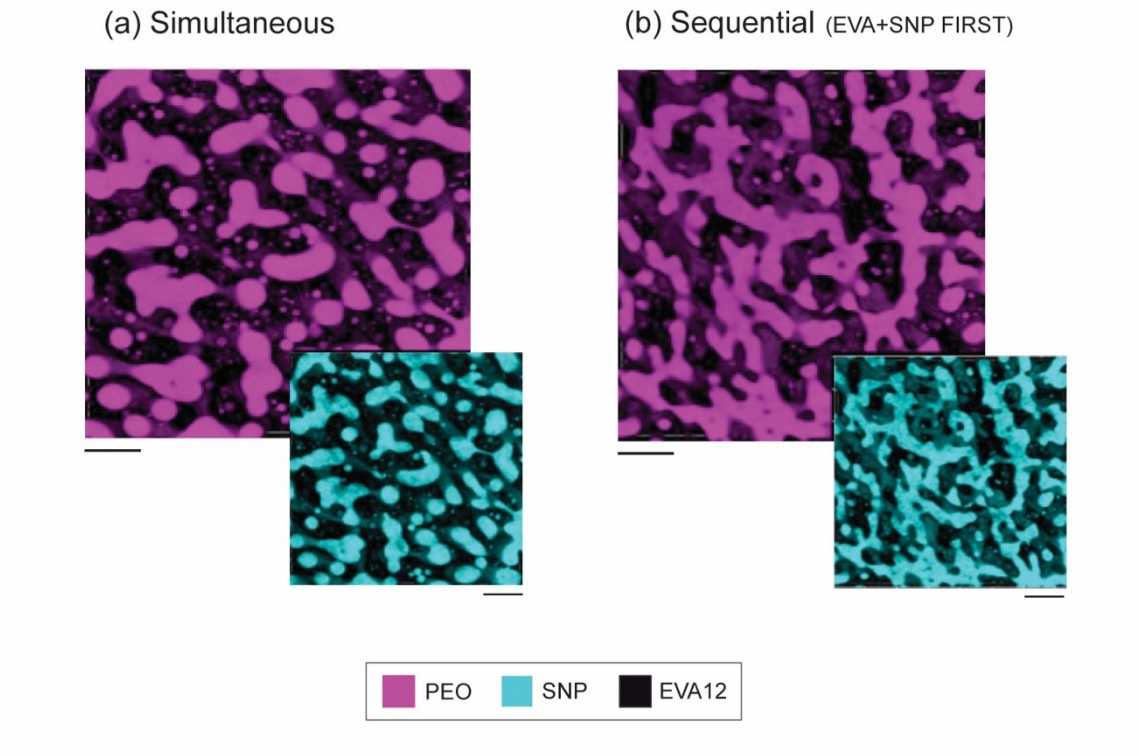

Figure S4. LSCM images of EVA/PEO (50/50 vol%) blends filled with 20 wt% (28 vol% to PEO) SNPs after 30 min melt annealing; (a) Simultaneous blending; and (b) EVA and SNP are blended first. Scale bars are 20 μm.

Figure S5 shows LSCM images of PE/PEO (50/50 vol%) blends filled with 30 wt% (28 vol% to PEO) SNPs after 30 min melt annealing.

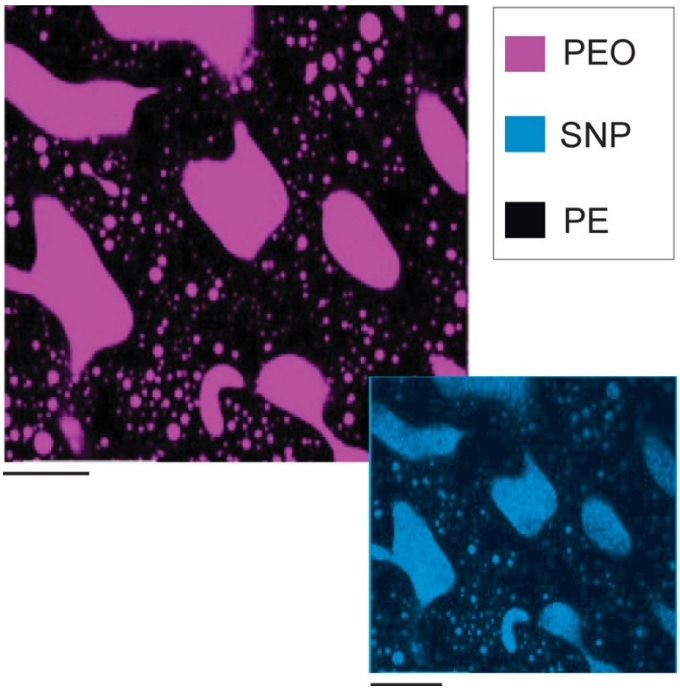

Figure S5. LSCM images of sequentially blended PE/PEO (50/50 vol%) (SNP+PE first) system filled with 30 wt% (28 vol% to PEO) SNPs after 30 min melt annealing. Scale bars are 50 μm.

Figure S6 illustrates the strain sweep data for the co-continuous and tri-continuous polymer blend nanocomposites [s7].

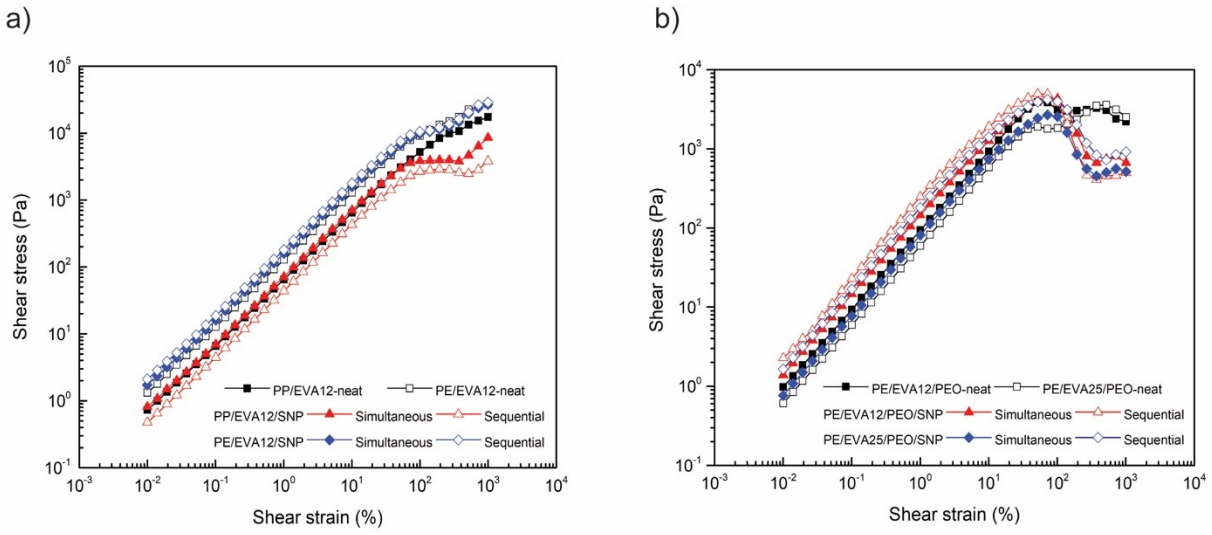

Figure S6. Shear stress vs. shear strain plot for a) neat binary blends and the co-continuous polymer blend nanocomposites, and b) neat ternary blends and tri-continuous polymer blend nanocomposites.

REFERENCES

(s1) Trifkovic, M.; Hedegaard, A. T.; Sheikhzadeh, M.; Huang, S.; Macosko, C. W. Stabilization of PE/PEO cocontinuous blends by interfacial nanoclays. *Macromolecules* **2015**, *48*, 4631−4644.

(s2) Occhiello, E.; Morra, M.; Morini, G.; Carbassi, F.; Johnson, D. On oxygen plasma-treated polypropylene interfaces with air, water, and epoxy resins. II. Epoxy resins. *J. Appl. Polym. Sci.* **1991**, *42*, 2045−2052.

(s3) Erbil, H. Y. Surface-free energy analysis of hydrolyzed ethylene-vinyl acetate copolymers. *J. Appl. Polym. Sci.* **1987**, *33*, 1397−1412.

(s4) Sang, C. L.; Seong, H. K.; Jung, H. L.; Mi, K. K.; Do, J. K.; Taehyoung, Z. Surface-treatment effects on organic thin-film transistors. *Synthetic Metals* **2005**, *148*, 75−79.

(s5) Canto, L.B. On the coarsening of the phase morphology of PP/EVA blends during compounding in a twin screw extruder. *Polymer Testing* **2014**, *34*, 175−182.

(s6) Elias, L.; Fenouillot, F.; Majeste, J. C.; Cassagnau, P. Morphology and rheology of immiscible polymer blends filled with silica nanoparticles. *Polymer* **2007**, *48*, 6029−6040.

(s6) Coussot, P. "Rheological aspects of the solid-liquid transition in jammed systems." *Jamming, Yielding, and Irreversible Deformation in Condensed Matter*. Berlin, Heidelberg: Springer-Verlag, 2006. 69-90.